Title
NMR Studies of Block Copolymer-Based Supramolecules in Solution

Journal
ACS Macro Letters, 9(7)

ISSN
2161-1653

Authors
Chang, Boyce S
Ma, Le
He, Mengdi
et al.

Publication Date
2020-07-21

DOI
10.1021/acsmacrolett.0c00434

NMR studies of Block Copolymer-Based Supramolecules in Solution

Boyce Chang†, Le Ma†, Mengdi He†, Ting Xu†‡*

† Department of Materials Science and Engineering, University of California, Berkeley, Berkeley, California 94720, United States

‡Materials Science Division, Lawrence Berkeley National Laboratory, Berkeley, California 94720, United States

Abstract

Hierarchical assemblies from block copolymer (BCP)-based supramolecules have shown immense potential as programmable materials owing to ease to incorporate functional molecules and to access array of hierarchical structures. However, there remains a knowledge gap on the formation of the supramolecule in solution. Here, we applied NMR techniques to investigate the solution phase behavior of the most studied supramolecular systems, polystyrene-*block*-poly(4-vinyl pyridine)(3-pentadecylphenol) (PS-*b*-P4VP(PDP)$_r$). The results show that the supramolecule adopts a coil-comb conformation despite the small molecule's (PDP) rapid exchange between the bonded and free states. The exchange rate (>10^4 s^{-1}) exceeds the NMR timescale at the frequency of interest. The supramolecules form under dilute conditions studied (~2vol%) and is attributed to the enthalpic gain of the hydrogen bonding between the PDP and 4VP. As the solute concentration increases (>10vol%), the supramolecule forms micelle-like aggregates with PDP accumulated within the comb-block's pervaded volume based on analysis of the apparent molecular weight, viscosity and chain dynamics as a function of solute concentration. This work sheds light on the long-standing question regarding the evolution of the

constituents in BCP-based supramolecule in solution and provides valuable guidance towards their solution-based processing and morphological control.

Introduction

The versatility of block copolymer (BCP)-based supramolecules have led to a plethora of hierarchical assemblies[1-6] to organize organic semiconductors,[7-8] form stimuli responsive composites[7] and photonic crystals.[9] The prime characteristic of BCP-based supramolecules is the attachment of mesogens onto the polymer side groups. This enables versatile control over the self-assembly and implementation of functional groups for targeted applications.[1] Given the volatility and weak interaction of small molecules, BCP-based supramolecules are typically not suitable for high temperature processing for polymer melts and/or polymer thin films. Instead, solution processing offers additional advantages such as rapid fabrication at room temperature and at low viscosity.[10] Furthermore, solvent vapor annealing expands the ability to tune morphology and access kinetically trapped phases.[11-14]

A detailed study on the solvent annealing parameters of polystyrene-b-poly(4-vinylpyridine) (3-pentadecylphenol)$_r$, PS-P4VP(PDP)$_r$ coil-comb supramolecular thin films revealed the importance of overall mobility and suggested the flexibility provided by the small molecule distribution to maintain order (r is the molar ratio of PDP relative to 4VP monomer).[15] In contrast, simulation and small angle X-ray scattering (SAXS) experiments on analogous supramolecular melts have demonstrated that the hydrogen bonded (H-bond) small molecules behave like permanent combs blocks.[16-17] Despite numerous efforts in characterizing supramolecule melt at elevated temperature above the BCP order-disorder transition temperature, challenges in quantifying the degree of H-bonding and distribution of small molecules remain

unsolved.[2, 18] Further questions on the chain conformation at different stages of the formation and self-assembly of supramolecules also persist, which could dictate energetic contribution and microdomain size from the comb-block. Efforts to obtain spatial information from SAXS is limited in disordered phases while the use of FTIR suffer from peak overlap and unreliable quantification.[1-2, 18] Aside from the challenges above, solution studies are subjected to additional complications. Using the same techniques, supramolecules in diluted solution typically yield lower signal to noise ratio and are subject to experimental constraints due to volatility of the solvent.

Nuclear magnetic resonance (NMR) spectroscopy is routinely used to characterize molecules in solution and to probe the changes in the local chemical environment of different moieties.[19] Dipolar interactions can be used to probe the spatial proximity of intermolecular moieties through the Nuclear Overhauser Effect (NOE). There are additional considerations and potential benefits to probe macromolecules due to their slow dynamics that leads to peak broadening and overlap. Characteristic changes to the dynamics of the system at various scales (between μs-ns) can be detected through NMR relaxometry and diffusion ordered (DOSY) experiments.[20-22]

Here, NMR spectroscopy is used to study the H-bonding of PDP onto the PS-P4VP BCP in solution as a function of solute concentration and the PDP:4VP ratio, r. The results confirmed that PDP is largely dynamic in solution, rapidly exchanging between the free and bonded states at rates, $k>10^4$ s^{-1}. Near complete occupancy of PDP on pyridine sites is achieved at solute concentrations as low as ~10vol%. Despite the constant exchange of the PDP molecules, the conformation of the P4VP block transitions from coil to comb when sufficient (>50%) pyridine

sites are H-bonded. Furthermore, the supramolecule chains were found to reach an aggregation-like state between solute concentration of 15-20vol%.

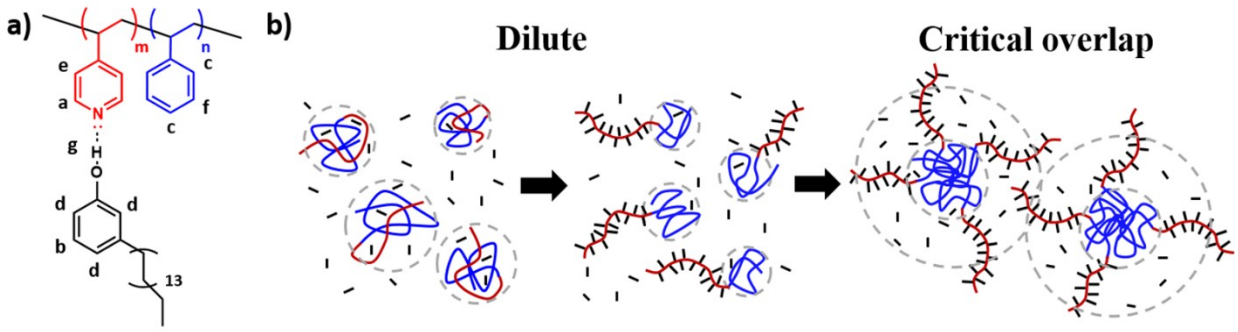

Figure 1. a) Chemical structure of PS-b-P4VP(PDP)$_1$ supramolecule. b) Schematic of small molecule attachment and conformation induced assembly at the critical overlap concentration in coil-comb supramolecules. (Blue: PS, Red: P4VP, Black: PDP)

Results and discussion

^{1}H NMR was used to study the formation of the supramolecule in solution by probing changes in hydrogen bonding, spatial proximity, and supramolecule's molecular weight. Chloroform is commonly used in solution processing of PS-P4VP(PDP)$_r$ because it has good solubility for each component, and thus, will be utilized as the solvent throughout this work. The supramolecule was constructed using a di-BCP, PS(33,000)-b-P4VP(8,000) and PDP at r=2 where r is the molar ratio between PDP and P4VP monomers (abbreviated as 33-8(2)). Proton spectra were obtained at supramolecule concentrations of 2, 5, 10, and 40vol%, respectively. As expected, the PDP hydroxyl protons are deshielded with increasing solute concentration (Figure 2a, S3). This is indicative of hydrogen bonding, however, the protons in the pyridine N···HO and in PDP O···HO are indistinguishable and only a single peak was observed. Based on the pKa of

protonated pyridine (5.2) and phenol (-2),[23] the former is likely to dominate hydrogen bonding. However, the use of pKa for estimating the extend of hydrogen bonding is complex for macromolecules due to steric hindrance and limited chain conformations.[24] Comparing supramolecules (PS-P4VP(PDP)$_r$) and pure PDP as a function of concentration shows both larger chemical shifts and slope (Figure S1). When excess PDP was used, as r is varied from 0.5 to 3.0, only a single OH signal was observed suggesting rapid chemical exchange rates between free and hydrogen bonded molecules.

The degree of occupancy of pyridine sites was measured using ^{1}H 1D Nuclear Overhauser Effect (NOE) with excitation focused on the pyridine *meta*-protons (*a*) due to their spatial proximity with the hydroxyl protons (*g*) of H-bonded PDP (Figure S3). NOE ratio is obtained by dividing the NOE signals from protons *a-g*, which are produced only by H-bonded sites, with *a-e*, signals present from all pyridine sites. Thus, it is a function of both interproton distance, r and fraction of H-bonded PDP (Figure 2b). [25] Assuming that the interproton distance ratio between *a-g* and *a-e* remains constant with increasing solute concentration, the NOE ratio becomes directly proportional to the fraction of H-bonded sites. Hence, the asymptotic trendline can be exploited to indicate the saturation point where all pyridine sites are occupied (Figure 2b). Varying PDP ratio (r=0.5-2) of the supramolecule at 15vol%, where the saturation begins validates the applicability of the trendline (Figure S4). Maxwell-Boltzmann statistics, $N_i = \exp\left(\frac{G}{kT}\right)$ was employed to gain further insight on the thermodynamic driving forces of supramolecule formation.[26] The number of PDP molecules at a given state, N_i is taken as the Boltzmann factor with respect to the Gibbs free energy, G. The change in enthalpy, ΔH is given as the heat of H-bond formation considering that hydrophobic contributions, which is

proportional to $\sqrt{X_d(1-f_s)}$, where X_d is the hydrophobic component of the Flory-Huggins parameter and f_s is the solvent fraction, are largely mitigated in the presence of chloroform.[10, 14, 27] Hansen solubility parameters are tabulated in the supporting information to highlight that hydrogen bonding and polar contributions are less affected by chloroform compared to van der Waals forces (Table S1). The change in entropy, ΔS constitutes both translational, ΔS_{trans} and conformational, ΔS_{con}. ΔS_{trans} can be modelled by mixing entropy as a function of small molecule volume fraction, $\Delta S_{mix}=k\ln(\varphi)$ while ΔS_{con} is calculated from entropic penalties by chain stretching. The latter term, however, only contributes ~0.15 kT per monomer/PDP based on entropic spring constant (Detailed calculations provided in the SI section S4-S5).[28] Thus, the data was fit solely based on mixing entropy. The predicted ΔH of ~7.5 kT conforms with reported values in literature for the enthalpy of alcohol-pyridine H-bonds (5-12 kT).[29-31] Furthermore, reasonable agreement (R^2=0.91) between the data and fitted curve suggest that translational entropy is likely the driving force for the PDP-pyridine separation.

^{13}C spin lattice relaxation (T_1) was used to probe changes in chain conformation. Since segmental dynamics is the principle mechanism for ^{13}C T1 relaxation, this method has been applied to study polymer conformations whereby stretched or restricted chains demonstrate higher values compared to amorphous random coils.[32-33] By probing the T_1 relaxation time of both PS and P4VP blocks at various concentrations (Table 1-2), relative changes in chain dynamics can be used to infer their conformations.[32-33] Analyzing the T_1 ratio of the pure BCP, which is taken as the ratio between T_1 relaxation of *meta*-C of P4VP (149 ppm)[34] and PS (127 ppm)[35] (*a* vs *f* Figure 1a), it was found that they shared equal relaxation times (T_1 ratio = 1) at concentrations below 20vol% (Figure 2d). A ^{13}C NMR spectrum of the 33-8(2) supramolecule is

provided in the supporting information. For a coil-coil chain conformation, the two blocks occupy similar environments, hence, exhibit comparable dynamics. At higher concentrations, P4VP encounters greater secondary interaction compared to PS (evident in its higher glass transition temperature),[36] which leads to a rise in T_1 ratio. These asymmetric chains are likely phase separated to form disordered micelle-like aggregates.[37-42]

T_1 relaxation time of polymer chains collected in high field spectrometers can be described by the following equation: $\frac{1}{T_1} \approx \tau_s + \tau_l^{-1/2}\omega^{-3/2}$ where τ_s is the segmental correlation time, τ_l is the mean diffusion time over correlation length, l and ω is the Larmor frequency.[21] τ_s is characterized by segmental motions at length scales below the Kuhn length, b while τ_l describes the relaxation time of reptative displacements within its pervaded volume at length scales significantly smaller than the chain length.[21, 43] Considering that $\tau_l > \tau_s \sim 1$ ns, and measurements were collected at high frequencies (600 MHz spectrometer), both terms could contribute significantly to T_1. However, the net rise in T_1 of P4VP and PS indicates that τ_l is dominant compared to τ_s because the loss of solvent leads to slower dynamics, thus increasing time at both length scales.

Comparing T_1 ratio between carbons *a* and *f* in the supramolecule, demonstrated greater T_1 ratio at all concentrations between 10-40vol%. The higher T_1 ratio at low concentrations is attributed to a conformational change of the P4VP block to a stretched comb, thus, increasing τ_l by restricting its reptative motions.[21] Additionally, the rise in T_1 ratio with increasing concentration was triggered at a lower concentration compared to the BCP, indicating a greater driving force for phase separation between the two blocks. The enhanced asymmetry in the comb block likely promotes micelle-like aggregation.[37-42]

Table 1. ^{13}C T_1 relaxation times of components in PS-P4VP BCP (33-8(0)) at different solute concentrations.

Concentration (%)	T_1 (ms), P4VP (149 ppm)	T_1 (ms), PS (127 ppm)	T_1 ratio
10	297 ± 9	299 ± 1	1.00
15	303 ± 5	303 ± 1	1.00
20	304 ± 8	302 ± 1	1.01
30	383 ± 15	320 ± 1	1.20

Table 2. ^{13}C T_1 relaxation times of components in PS-P4VP$(PDP)_2$ (33-8(2)) supramolecule at different solute concentrations.

Concentration (%)	T_1 (ms), P4VP (149 ppm)	T_1 (ms), PS (127 ppm)	T_1 ratio
10	337 ± 28	287 ± 1	1.17
15	350 ± 26	289 ± 1	1.21
20	387 ± 10	288 ± 1	1.34
40	512 ± 15	334 ± 1	1.54

Changes in the dynamics of PDP was examined using its diffusion length, *L*, which is the longest distance a free PDP molecule can travel before exchanging with a bonded PDP, as a function of concentration using the equation $L=\sqrt{Dt}$ (Figure 2e). Here, *D* is the diffusion constant measured by diffusion ordered NMR spectroscopy (DOSY) and *t* is the maximum lifetime of the PDP in motion. *t* is calculated by treating the observed PDP hydroxyl protons (*g*) as a collapsed peak between free and bonded PDP due to rapid exchange rates. Hence, the

following equation for maximum lifetime, $t = \frac{1}{\sqrt{2}\pi\Delta\upsilon}$ where Δυ is the frequency difference between free and bonded PDP, which is approximated as twice the frequency difference (from chemical shift) of *g* protons between pure PDP and the supramolecule (result of exchange between free and bonded PDP) (Figure S1).[44] The value of *t* was observed to be on the order of 100 μs meaning that the PDP exchange rate exceeds 10^4 s^{-1}. From the maximum distance travelled by free PDP, *L*, a spherical diffusion volume, V_D can be calculated by taking *L* as the radius (Figure 2f). Interestingly, V_D closely matched the shrinkage in global volume at dilute concentrations and begin to deviate above 10vol%, which coincides with the formation of the comb-block. Considering that H-bonding occurs below that concentration, the formation of the supramolecule did not significantly affect its average mobility. Hence, the deviation in V_D above 10vol% represents a biased among the free PDP molecules to reside in the vicinity of the comb-block. This result further hints at the phase separation between the two blocks above 10vol%.

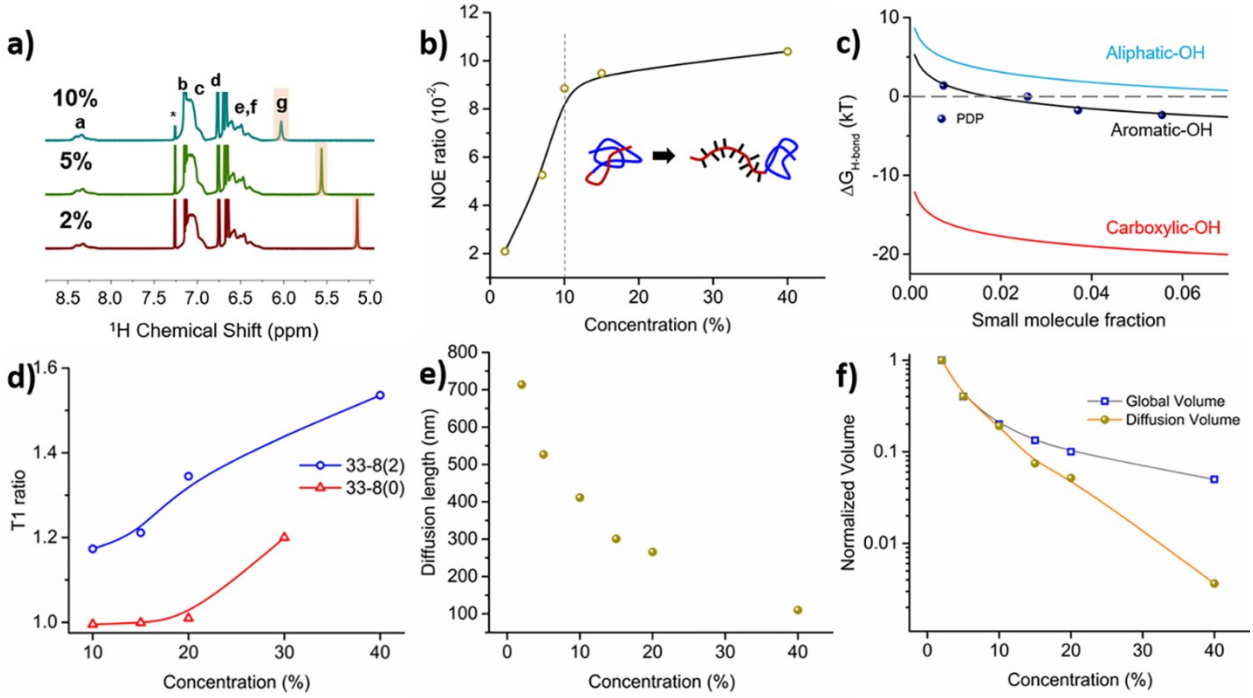

Figure 2. a) ^{1}H NMR spectra of the supramolecule (33-8(2)) at different concentrations. PDP hydroxyl protons are highlighted. b) 1D gradient selective ^{1}H NOE ratio between pyridine and PDP hydroxyl protons. c) Gibbs free energy of supramolecule formation estimated using Maxwell-Boltzmann statistics for PDP and other small molecules using bond energies from literature. [30, 45] d) ^{13}C NMR T1 relaxation ratio between P4VP(*a*, 149 ppm- PS (*f*, 127 ppm) as a function of concentration. e-f) Maximum diffusion length and volume of PDP before undergoing bond exchange.

The deviation in V_D above 10vol% can be explained through analysis of the asymmetry between the two blocks. With respect to the critical overlap concentration for r=2, the comb-block forms at approximately the same concentration as the onset of chain entanglement among the PS blocks (Figure 3a). Asymmetry in fractal dimension, ~~Đ~~ of the PS coil (~~Đ~~=2) and P4VP(PDP) comb (~~Đ~~ = 1) necessitates an excluded volume surrounding the comb-block to maintain equal chain density in solution (Figure 3b).[28] At the critical overlap, the formation of entanglements drives aggregation of chains. The asymmetry between the two blocks could yield aggregates with two possible orientations: i) PS core with repulsive forces from the excluded volume in the comb-block forming discrete micellar aggregates (Figure 1b) or ii) PS block forms a continuous phase that envelops the comb-block core. The former will result in lower viscosity compared to the latter due to reduced overlap between aggregates.

In order to validate the presence of such aggregates and predict their sizes, DOSY was performed. Molecular weight, M_w was calculated using the scaling law between diffusion constant, D and M_w, $D \sim M_w^{-0.6}$ (Figure 3c) (Details of the calculations provided in the SI section S6).[46] The effects of solution viscosity was suppressed by normalizing all D values with the

solvent diffusion constant. However, attention should be given to the relative changes in M_w rather than absolute values considering the dilute assumption required for accurate M_w calculations using the Stokes-Einstein equation.[22] Under dilute concentrations (2-10vol%), the experimental values closely matched the predicted M_w of a growing supramolecule (calculated using the PDP attachment data in Figure 1b). Above 10vol%, a sharp increase in M_w was observed, which supports the formation of aggregates. Nevertheless, considering that the system is above its critical overlap concentration and assumptions in the Stokes-Einstein equation, the rise in M_w could be influenced by stark changes in viscosity.

Rapid changes in viscosity of polymer solutions are characterized by the transition from discrete chains to entangled networks.[28] Thus, measuring solution viscosity qualitatively probes the degree of entanglement in the system. Here, viscosity of the solution is calculated (Figure 3d) by tracking the diffusion constant of the solvent (Details of the calculations provided in the SI section S6). From 2-10vol%, the increased overlap between BCP chains (Figure 3a) is counteracted by the concomitant formation of the comb-block (Figure 2b), which reduces net entanglements leading to gradual increase in viscosity. Surprisingly, at the onset of M_w increment above 10vol%, a plateau in viscosity was observed, supporting the formation of discrete aggregates that are poorly intertwined. Thus, we propose that the aggregates consist of a highly entangled PS core while the weakly overlapped P4VP comb-block forms a continuous phase (inset Figure 3d). This orientation corroborates with the repulsion or lack of entanglements between aggregates as suggested by the plateau in viscosity between 10-20vol% (Figure 3d). The aggregation number, N_{agg} approximated as $N_{agg} = M_{w(exp)}/M_{w(predicted)}$, ranged between 6 - 22 in this region, which is lower compared to typical melt phase BCP micelles (~10^2).[39] This is attributed to the solvent molecules acting as the major component in this study, therefore, limiting the

number of chains per unit volume.DOSY was also performed on supramolecules with different PDP ratio to elucidate the role of chain conformation in the formation of such aggregates (Figure 3e). The concentration of the supramolecules were held at 15vol% to ensure that they exceed the critical overlap. At r = 0.5 where only half the pyridine sites are occupied by PDP, the experimental M_w falls within prediction indicating that no aggregates are formed. At r = 1 and above, M_w several times larger than the predicted value were obtained. The continued increase in size from r = 1 to 2 is ascribed to excess PDP molecules acting as plasticizers in the PS core causing it to swell.[15, 47] The expanded core caused the N_{agg} to increase from 7 to 22. However, the higher amount of free PDP could also improve the segregation strength between the two blocks, leading to fusion between aggregates.[48]

Given the low PDP ratio at r = 0.5 and the dynamic nature of the H-bond, there remain uncertainties toward the conformation of the P4VP(PDP) block. ^{13}C T_1 relaxation experiments (Figure 3f) confirms that the supramolecule remains coil-coil (P4VP/PS T_1 ratio = 1), identical to the native BCP at r=0.5. Subsequently, the T_1 ratio increased dramatically above r=0.5 and plateau above r=1, signifying a transition to coil-comb. The fact that T_1 ratio remained constant from r=0-0.5 validates that the changes probed are due to τ_1 because segmental dynamics, τ_s should theoretically scale with number of occupied P4VP sites. Finally, the viscosity trend shows an asymptotic decay above r=0.5, which confirms that the formation of discrete aggregates hinges on the fraction of hydrogen bonded pyridine side groups (Figure 3f). When r is reduced below a critical value (~0.7), the coil-comb architecture reverts to coil-coil, which disrupts the asymmetry between the two blocks and prevents the growth of discrete aggregates.

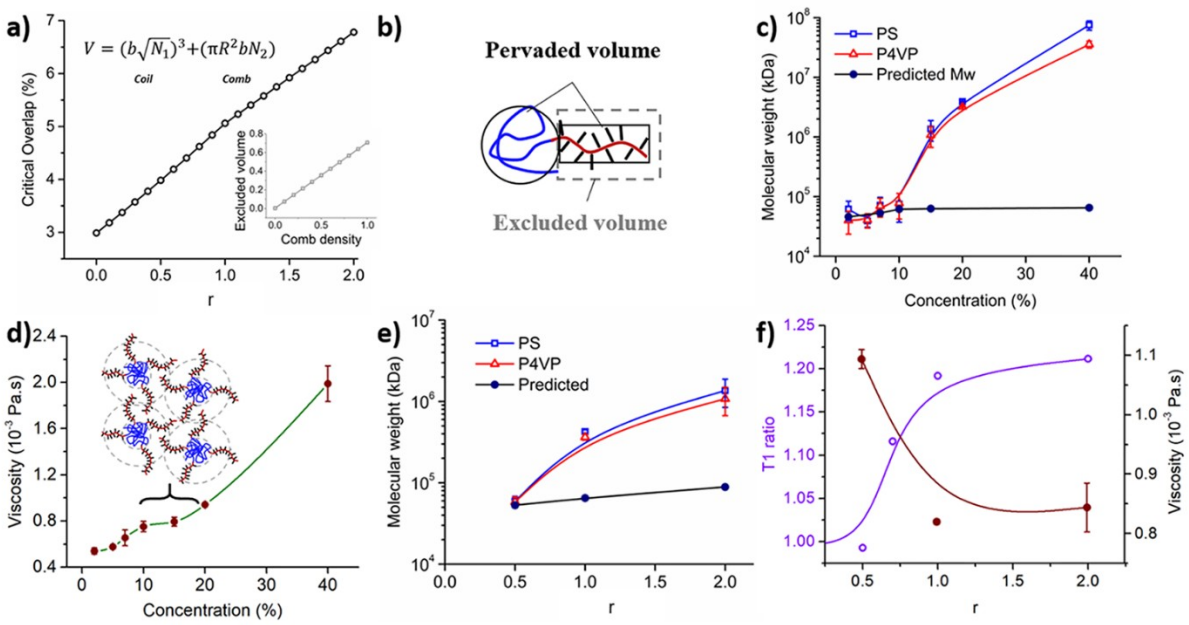

Figure 3. a) Calculated critical overlap concentration of supramolecule as a function of r, PDP:4VP ratio. b) Schematic of excluded volume in the comb-block as a result of fractal dimension asymmetry. c) Molecular weight of supramolecule as a function of concentration calculated from DOSY NMR. d) Viscosity of the corresponding solution estimated using solvent diffusion constants. e) Molecular weight of supramolecule as a function of r, PDP:4VP ratio at 15vol%. f) ^{13}C NMR T1 relaxation ratio between P4VP(*a*, 149 ppm- PS (*f*, 127 ppm)and viscosity as a function of r at 15vol%.

In conclusion, we demonstrate that the supramolecule adopts a coil-comb conformation in solution despite PDP molecules undergoing rapid exchange between bonded and free states. Attachment of the small molecule onto the BCP in solution is governed by translational entropy, indicating that a relatively high solvent volume percent is required for complete separation of the two species. Furthermore, PDP appears to be confined within the comb-block even at rather low solute concentration. Through a systematic analysis of molecular weight, viscosity and chain

dynamics as a function of concentration, we propose that the supramolecule forms micelle-like aggregates that consist of an entangled PS core and weakly overlapping P4VP(PDP) corona. The pseudo-phase separation would result in small molecules concentrated in the corona region. Furthermore, we establish the dependence of aggregation and formation of the coil-comb conformation on the fraction of P4VP side groups hydrogen bonded to PDP. This work deepens our understanding of the evolution of the constituents in BCP-based supramolecules in solution, the driving forces that govern assembly and provides valuable guidance toward solution-based processing.

Associated Content

Supporting information

The Supporting Information is available free of charge at

Detailed information on materials, experimental procedures, ^{1}H NMR of the BCP, proton chemical shift as a function of concentration, NOE as a function of PDP ratio, diffusion constants measured from DOSY and calculations used for plots presented in Figure 2 and Figure 3.

Author Information

Corresponding Author

Ting Xu – Department of Materials Science and Engineering, University of California–Berkeley, Berkeley, California 94720, United States; Materials Sciences Division, Lawrence Berkeley National Lab, Berkeley, California 94720, United States.

Author Contributions

The manuscript was written through contributions of all authors.

Notes

The authors declare no conflict of interest.

Acknowledgements

This work was funded by the U.S. Department of Energy, Office of Science, Office of Basic Energy Sciences, Materials Sciences and Engineering Division, under Contract DE-AC02-05-CH11231 (Organic–Inorganic Nanocomposites KC3104). We thank Dr. Hasan Celik and UC Berkeley's NMR facility in the College of Chemistry (CoC-NMR) for spectroscopic assistance. Instruments in the CoC-NMR are supported in part by NIH S10OD024998.

Reference

1. Ruokolainen, J.; Mäkinen, R.; Torkkeli, M.; Mäkelä, T.; Serimaa, R.; Brinke, G. t.; Ikkala, O., Switching Supramolecular Polymeric Materials with Multiple Length Scales. *Science* **1998,** *280* (5363), 557.
2. Ruokolainen, J.; Saariaho, M.; Ikkala, O.; ten Brinke, G.; Thomas, E. L.; Torkkeli, M.; Serimaa, R., Supramolecular Routes to Hierarchical Structures: Comb-Coil Diblock Copolymers Organized with Two Length Scales. *Macromolecules* **1999,** *32* (4), 1152-1158.
3. Pollino, J. M.; Weck, M., Non-covalent side-chain polymers: design principles, functionalization strategies, and perspectives. *Chemical Society Reviews* **2005,** *34* (3), 193-207.
4. Kao, J.; Xu, T., Nanoparticle Assemblies in Supramolecular Nanocomposite Thin Films: Concentration Dependence. *Journal of the American Chemical Society* **2015,** *137* (19), 6356-6365.
5. Thünemann, A. F.; Kubowicz, S.; Burger, C.; Watson, M. D.; Tchebotareva, N.; Müllen, K., α-Helical-within-Discotic Columnar Structures of a Complex between Poly(ethylene oxide)-block-poly(l-lysine) and a Hexa-peri-hexabenzocoronene. *Journal of the American Chemical Society* **2003,** *125* (2), 352-356.
6. da Silva, R. M. P.; van der Zwaag, D.; Albertazzi, L.; Lee, S. S.; Meijer, E. W.; Stupp, S. I., Super-resolution microscopy reveals structural diversity in molecular exchange among peptide amphiphile nanofibres. *Nature Communications* **2016,** *7* (1), 11561.
7. Zhao, Y.; Thorkelsson, K.; Mastroianni, A. J.; Schilling, T.; Luther, J. M.; Rancatore, B. J.; Matsunaga, K.; Jinnai, H.; Wu, Y.; Poulsen, D.; Fréchet, J. M. J.; Paul

Alivisatos, A.; Xu, T., Small-molecule-directed nanoparticle assembly towards stimuli-responsive nanocomposites. *Nature Materials* **2009,** *8* (12), 979-985.
8. Tung, S.-H.; Xu, T., Templated Assembly of Block Copolymer toward Nonequilibrium Nanostructures in Thin Films. *Macromolecules* **2009,** *42* (15), 5761-5765.
9. Valkama, S.; Kosonen, H.; Ruokolainen, J.; Haatainen, T.; Torkkeli, M.; Serimaa, R.; ten Brinke, G.; Ikkala, O., Self-assembled polymeric solid films with temperature-induced large and reversible photonic-bandgap switching. *Nature Materials* **2004,** *3* (12), 872-876.
10. Kao, J.; Thorkelsson, K.; Bai, P.; Zhang, Z.; Sun, C.; Xu, T., Rapid fabrication of hierarchically structured supramolecular nanocomposite thin films in one minute. *Nature Communications* **2014,** *5* (1), 4053.
11. van Zoelen, W.; Polushkin, E.; ten Brinke, G., Hierarchical Terrace Formation in PS-b-P4VP(PDP) Supramolecular Thin Films. *Macromolecules* **2008,** *41* (22), 8807-8814.
12. van Zoelen, W.; Asumaa, T.; Ruokolainen, J.; Ikkala, O.; ten Brinke, G., Phase Behavior of Solvent Vapor Annealed Thin Films of PS-b-P4VP(PDP) Supramolecules. *Macromolecules* **2008,** *41* (9), 3199-3208.
13. Huang, J.; Xiao, Y.; Xu, T., Achieving 3-D Nanoparticle Assembly in Nanocomposite Thin Films via Kinetic Control. *Macromolecules* **2017,** *50* (5), 2183-2188.
14. Huang, J.; Qian, Y.; Evans, K.; Xu, T., Diffusion-Dependent Nanoparticle Assembly in Thin Films of Supramolecular Nanocomposites: Effects of Particle Size and Supramolecular Morphology. *Macromolecules* **2019,** *52* (15), 5801-5810.
15. Evans, K.; Xu, T., Self-Assembly of Supramolecular Thin Films: Role of Small Molecule and Solvent Vapor Annealing. *Macromolecules* **2019,** *52* (2), 639-648.
16. Huh, J.; Ikkala, O.; ten Brinke, G., Correlation Hole Effect in Comblike Copolymer Systems Obtained by Hydrogen Bonding between Homopolymers and End-Functionalized Oligomers. *Macromolecules* **1997,** *30* (6), 1828-1835.
17. Huh, J.; Ikkala, O.; Ten Brinke, G., Correlation hole effect in comblike copolymer systems obtained by hydrogen bonding between homopolymers and end-functionalized oligomers. *Macromolecular Symposia* **1997,** *121* (1), 123-131.
18. Hofman, A. H.; Reza, M.; Ruokolainen, J.; ten Brinke, G.; Loos, K., The Origin of Hierarchical Structure Formation in Highly Grafted Symmetric Supramolecular Double-Comb Diblock Copolymers. *Macromolecular Rapid Communications* **2017,** *38* (17), 1700288.
19. Günter, H., *NMR spectroscopy*. 1995; Vol. 2.
20. Cohen, Y.; Slovak, S., Diffusion NMR for the characterization, in solution, of supramolecular systems based on calixarenes, resorcinarenes, and other macrocyclic arenes. *Organic Chemistry Frontiers* **2019,** *6* (10), 1705-1718.
21. Kimmich, R.; Bachus, R., NMR field-cycling relaxation spectroscopy, transverse NMR relaxation, self-diffusion and zero-shear viscosity: Defect diffusion and reptation in non-glassy amorphous polymers. *Colloid and Polymer Science* **1982,** *260* (10), 911-936.
22. Li, W.; Chung, H.; Daeffler, C.; Johnson, J. A.; Grubbs, R. H., Application of 1H DOSY for Facile Measurement of Polymer Molecular Weights. *Macromolecules* **2012,** *45* (24), 9595-9603.
23. Solomons, T., *Fundamentals of organic chemistry*. 1997.

24. Savage, H. J.; Elliott, C. J.; Freeman, C. M.; Finney, J. L., Lost hydrogen bonds and buried surface area: rationalising stability in globular proteins. *Journal of the Chemical Society, Faraday Transactions* **1993,** *89* (15), 2609-2617.
25. Jones, C. R.; Butts, C. P.; Harvey, J. N., Accuracy in determining interproton distances using Nuclear Overhauser Effect data from a flexible molecule. *Beilstein J Org Chem* **2011,** *7*, 145-150.
26. DeHoff, R., *Thermodynamics in materials science*. CRC Press: 2006.
27. Jung, Y. S.; Ross, C. A., Solvent-Vapor-Induced Tunability of Self-Assembled Block Copolymer Patterns. *Advanced Materials* **2009,** *21* (24), 2540-2545.
28. Rubinstein, M.; Colby, R. H., *Polymer physics*. Oxford university press New York: 2003; Vol. 23.
29. Spencer, J. N.; Andrefsky, J. C.; Grushow, A.; Naghdi, J.; Patti, L. M.; Trader, J. F., Hydrogen bond equilibria of phenol-pyridine in cyclohexane, carbon tetrachloride, and benzene solvents. *The Journal of Physical Chemistry* **1987,** *91* (6), 1673-1674.
30. Adam, W.; Grimison, A.; Hoffmann, R.; Zuazaga de Ortiz, C., Hydrogen bonding in pyridine. *Journal of the American Chemical Society* **1968,** *90* (6), 1509-1516.
31. Lomas, J. S.; Maurel, F., Water and alcohol(s): what's the difference? A proton NMR and DFT study of hetero-association with pyridine. *Journal of Physical Organic Chemistry* **2008,** *21* (6), 464-471.
32. Schilling, F. C.; Sozzani, P.; Bovey, F. A., Chain conformation and dynamics of crystalline 1,4-trans-polyisoprene and its inclusion compound with perhydrotriphenylene. *Macromolecules* **1991,** *24* (15), 4369-4375.
33. Giotto, M.; Azar, D.; Gosselin, J.; Inglefield, P. T.; Jones, A. A., An NMR study of mobility in a crystalline side-chain comblike polymer. *Journal of Polymer Science Part B: Polymer Physics* **2001,** *39* (13), 1548-1552.
34. Wang, W.; Zhao, J.; Yu, H.; Zhou, N.; Zhang, Z.; Zhu, X., Simultaneously improving controls over molecular weight and stereoregularity of Poly(4-vinylpyridine) via a hydrogen bonding-facilitated controlled radical polymerization. *Polymer* **2013,** *54* (13), 3248-3253.
35. Wu, Y.-C.; Kuo, S.-W., Complementary multiple hydrogen bonding interactions mediate the self-assembly of supramolecular structures from thymine-containing block copolymers and hexadecyladenine. *Polymer Chemistry* **2012,** *3* (11), 3100-3111.
36. Mark, J. E., *Polymer Data Handbook*. Oxford University Press: 1999.
37. Hashimoto, T.; Kumaki, J.; Kawai, H., Time-resolved light scattering studies on kinetics of phase separation and phase dissolution of polymer blends. 1. Kinetics of phase separation of a binary mixture of polystyrene and poly(vinyl methyl ether). *Macromolecules* **1983,** *16* (4), 641-648.
38. Han, C. D.; Vaidya, N. Y.; Kim, D.; Shin, G.; Yamaguchi, D.; Hashimoto, T., Lattice Disordering/Ordering and Demicellization/Micellization Transitions in Highly Asymmetric Polystyrene-block-Polyisoprene Copolymers. *Macromolecules* **2000,** *33* (10), 3767-3780.
39. Wang, X.; Dormidontova, E. E.; Lodge, T. P., The Order−Disorder Transition and the Disordered Micelle Regime for Poly(ethylenepropylene-b-dimethylsiloxane) Spheres. *Macromolecules* **2002,** *35* (26), 9687-9697.
40. Schwab, M.; Stühn, B., Thermotropic Transition from a State of Liquid Order to a Macrolattice in Asymmetric Diblock Copolymers. *Physical Review Letters* **1996,** *76* (6), 924-927.

41. Abuzaina, F. M.; Patel, A. J.; Mochrie, S.; Narayanan, S.; Sandy, A.; Garetz, B. A.; Balsara, N. P., Structure and Phase Behavior of Block Copolymer Melts near the Sphere−Cylinder Boundary. *Macromolecules* **2005,** *38* (16), 7090-7097.
42. Kinning, D. J.; Winey, K. I.; Thomas, E. L., Structural transitions from spherical to nonspherical micelles in blends of poly(styrene-butadiene) diblock copolymer and polystyrene homopolymers. *Macromolecules* **1988,** *21* (12), 3502-3506.
43. Kimmich, R.; Rosskopf, E.; Schnur, G.; Spohn, K. H., Chain dynamics and molecular weight dependence of carbon-13 and hydrogen-1 relaxation times in polystyrene and polyethylene melts. *Macromolecules* **1985,** *18* (4), 810-812.
44. Bryant, R. G., The NMR time scale. *Journal of Chemical Education* **1983,** *60* (11), 933.
45. Gilli, P.; Pretto, L.; Bertolasi, V.; Gilli, G., Predicting Hydrogen-Bond Strengths from Acid−Base Molecular Properties. The pKa Slide Rule: Toward the Solution of a Long-Lasting Problem. *Accounts of Chemical Research* **2009,** *42* (1), 33-44.
46. Hiemenz, P. C.; Lodge, T. P., *Polymer chemistry*. CRC press: 2007.
47. Valkama, S.; Ruotsalainen, T.; Nykänen, A.; Laiho, A.; Kosonen, H.; ten Brinke, G.; Ikkala, O.; Ruokolainen, J., Self-Assembled Structures in Diblock Copolymers with Hydrogen-Bonded Amphiphilic Plasticizing Compounds. *Macromolecules* **2006,** *39* (26), 9327-9336.
48. Mysona, J. A.; McCormick, A. V.; Morse, D. C., Mechanism of Micelle Birth and Death. *Physical Review Letters* **2019,** *123* (3), 038003.

TOC